VOLUME 198, Nos. 1–3
APRIL I 1994

ISSN 0921–4526

PHYSICA B

CONDENSED MATTER

Proceedings of the International Conference on Surface X-Ray and Neutron Scattering

SXNS-3

held in Dubna, Russia
24–29 June 1993

Guest Editors:
H.J. Lauter
V.V. Pasyuk

PHYBE3 198 (1–3) 1–266 (1994)

NORTH-HOLLAND

ELSEVIER

Physica B 198 (1994) 150-155

PHYSICA

Forward scattering of neutrons from polymeric and magnetic multilayers

G.P. Felcher

Argonne National Laboratory, Argonne, IL 60439, USA

Abstract

Grazing incidence neutrons are not only reflected and refracted from imperfect layers, but also partially scattered by lateral dishomogeneities. In general, scattering may take place both in the reflection plane ("forward scattering") and out of it. The forward scattering from multilayers is highly structured in ridges, whose maxima can be indexed in terms of the multilayer spacings. In experiments on diverse diblock copolymers, two kinds of ridges were found, either at constant-k_z loci or else at constant-q_z loci. The relative intensity of the ridges appears to be related to the type and size of imperfections of the lamellar structure. Constant-q_z streaks of magnetic nature were also found in the forward scattering of metallic superlattices (Fe/Cr, Co/Ru, Fe/Nb) in the antiferromagnetic state. Here the diffuse scattering appears around the antiferromagnetic peaks while they are absent from the structural peaks, as if the crystalline superlattice were to partition into antiferromagnetic domains of limited lateral extension and columnar character.

Introduction

In grazing incidence geometry neutrons are either refracted or specularly reflected from an exactly planar sample. At an angle of incidence θ_i, and for a neutron wavelength λ, the component of the incident wave vector perpendicular to their surface is $k_{zi} = 2\pi \sin\theta_i/\lambda$. Similarly, for the exit beam $k_{zf} = 2\pi \sin\theta_f/\lambda$. The scattering vector is simply $q_z = k_{zi} + k_{zf}$. From the intensity reflected as a function of q_z the depth profile of the material may be obtained with great accuracy [1, 2]. When the sample's planes are not perfect (because the surface or some interfaces are rough, or the layers are undulated, or the layers are marred by impurities), neutrons are also scattered: the scattering may take place in the plane of reflection (defined by the angle of incidence θ_i and reflection θ_f), or else at an angle $\Delta\phi$ out of the reflection plane. By applying the conditions of conservation of energy and momentum it is easy to see [3, 4] that in the former type of scattering objects up to a size of the order of several microns can be observed. These objects are two orders of magnitude larger than those observable in other small angle scattering geometries. The present note is concerned with the phenomenology of this kind of scattering – which shall be named *forward scattering* – from imperfect multilayers.

The data presented here were collected at two POSY reflectometers [5] at the Intense Pulsed Neutron Source at Argonne National Laboratory. In both instruments a pulsed beam of neutrons, of all wavelengths in the thermal range, are brought onto the sample at an angle θ_i. Position-sensitive detectors record the neutrons reflected at $\theta_f = \theta_i$ (as well as the scattered neutrons at $\theta_f \neq \theta_i$) as a function of their time-of-flight from the source, and thus of their wavelength. The detectors are position-sensitive only along one direction (increasing θ) and in practice integrate over $\Delta\phi$. Measurements were performed on polymers at the highly automated instrument POSY II. Magnetic multilayers were studied at the polarized neutrons reflectometer POSY I.

0921-4526/94/$07.00
SSDI 0921-4526(93)E0527-N

2. Polymeric multilayers

Figure 1 shows the forward scattering from a film made of symmetric, diblock copolymers of polystyrene (PS) and polymethylmethacrylate (PMMA), for short P(S-b-MMA). Thin films of P(S-b-MMA), cast onto silicon substrates, heated to temperatures above the glass transition temperature ($\sim 100°C$), microphase separate into a lamellar morphology [6, 7]. The lamellae are parallel to the film surface, and their thickness is given by $(n + 1/2)L$, where n is an integer and L is the periodicity of the layers (in this sample of molecular weight $\sim 10^5$, $L = 520$ Å). PMMA segregates to the substrate and PS to the air surface. The sample whose scattering is presented in Fig. 1 had a thickness of 3.410^3 Å which corresponds to an integer number of layers ($n = 6$) and thus, after annealing, did not show the islands or wells that form at the surface for an arbitrary film thickness [6]. However, a strong perturbation was introduced into the layering by mixing into P(S-b-MMA) 10% of pure PMMA ($M_w = 510^4$). Since PS and PMMA are not miscible, the homopolymer is expected to share the same volume of the PMMA portion of the copolymer. In order to enhance the optical contrast of the lamellae, hydrogen was substituted with deuterium in the PS block of the copolymer.

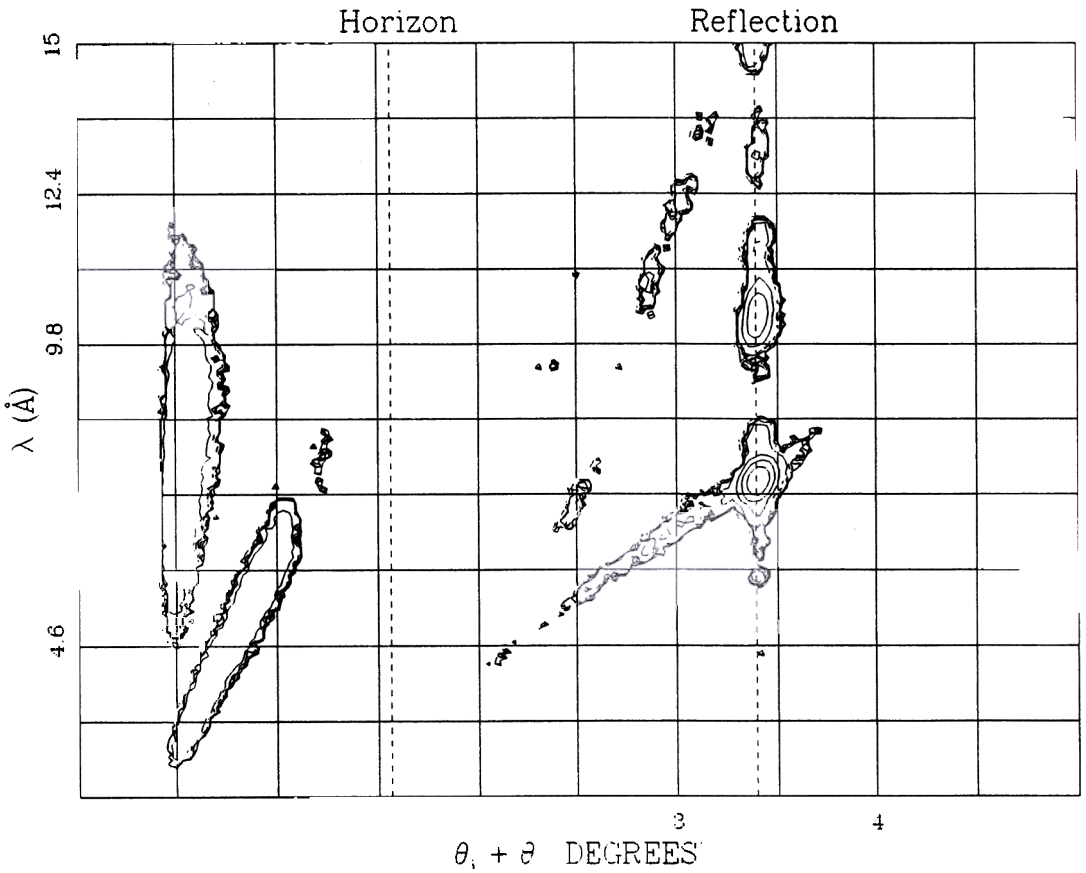

Fig. 1. Contour plot (on a log scale) of the intensities forwardly scattered from a sample of PS–PMMA copolymer containing 10% PMMA homolymer. The angle of incidence is $\theta_i = 1.58°$. The abscissa is $\theta_i + \theta_f$: $\theta_f = 0$ corresponds to the horizon of the sample surface; below this angle the neutrons are refracted from the sample, and exit from the edge of the substrate. The specularly reflected beam is located at $\theta_i = \theta_f$.

Figure 1 was obtained for an angle of incidence $\theta_i = 1.58°$. The abscissa is given in terms of the angle of scattering $\theta_i + \theta_f$ and the ordinate as the neutron wavelength. Although such a representation may appear clumsy and too linked to the geometry of the experiment, it is actually more readable than, for instance, a representation in the q space (q is the momentum transfer in vacuum, with coordinates q_z, q_x). Well visible is the reflection line at $\theta_i = \theta_f$. The angle $\theta_f = 0$ corresponds to the surface horizon, which divides the neutrons scattered back in free space from those refracted into the substrate and exiting from its edge. As in a Laue camera, here the whole scattering spectrum is recorded: no features are missed, as may be the case when a single wavelength is used or a detector with a single position channel. Figure 2 shows the position of the local maxima obtained at each wavelength, just for the neutrons scattered above the horizon. In Fig. 2 are presented as well the loci of the maxima from runs at $\theta_i = 0.6°$ and 1.05°. All the datapoints fall on simple patterns, to be interpreted with the help of the specular reflectivity [8].

The specularly reflected intensity is presented in the inset of Fig. 2. Maxima are visible at the critical momentum ($q_{zc} = 0.012$ Å^{-1}) and at $q_{z1} = 0.0208$, $q_{z2} = 0.0336$ and $q_{z3} = 0.0468$ Å^{-1} (the difference between adjacent maxima, $\Delta q_z \sim 2\pi/L$, where L is the periodicity of the layer). The loci of the diffuse scattering maxima obey the simple relation

$$2\pi\sin\theta_f/\lambda = q_{zM}/2 = k_{zM}, \qquad (1)$$

where M takes one of the values given above. Equation (1) gives rise to the sets of straight lines ending up, for $\lambda = 0$, to θ_i; clearly, they are loci of the majority of datapoints. The constant-k_z scattering was first discovered a long time ago for $M = c$ by Yoneda [9] (for symmetry, k_z can be the exit or the

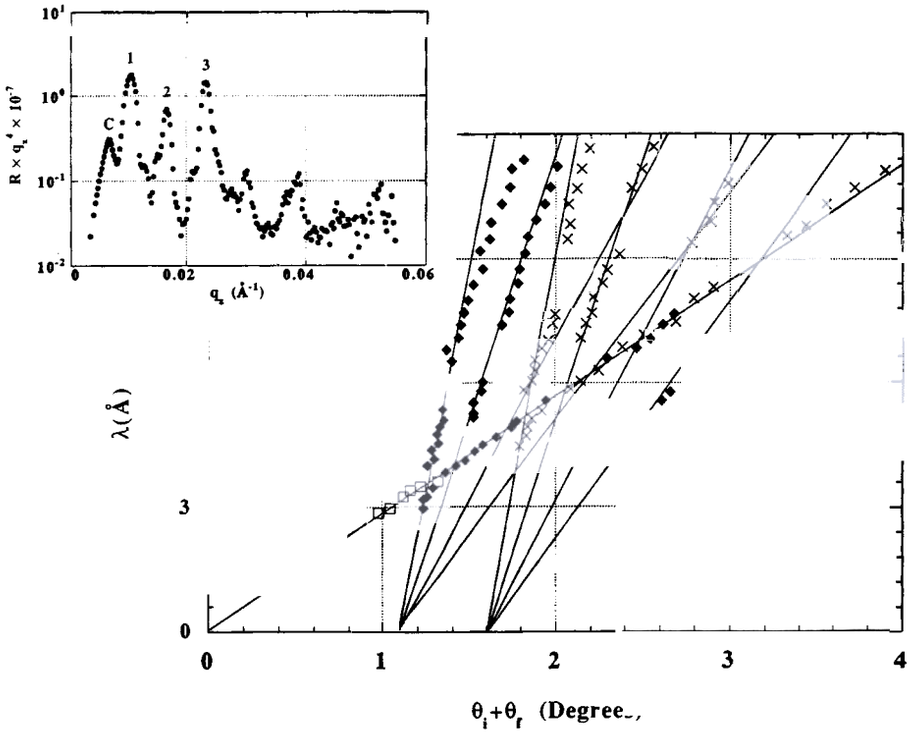

Fig. 2. Loci of the scattering maxima for the sample described in Fig. 1, at three different angles of incidence (for clarity, maxima relative to the specularly reflected beams have been omitted). In the chosen axes the constant-k_z lines become $[(\theta_i + \theta_f)/q_{zM} - \theta_i/q_{zM}] = \lambda/4\pi$. Constant-$q_z$ lines become $(\theta_i + \theta_f)/q_{zM} = \lambda/2\pi$. Inset: the reflectivity of the same sample (multiplied by q_z^4). Crosses: $\theta_i = 1.58°$; diamonds: $\theta_i = 1.05°$; open squares: $\theta_i = 0.6°$.

entrance beam), and recently "super Yoneda", or constant-k_{zM} scattering, has been observed for values of M indicating one of the interference maxima of the reflectivity [3]. The position of the ridges is independent of the angle of incidence θ_i; in other words, the memory of θ_i is lost and the indexing is done in terms of the wave vector of the exiting wave k_{zf} only. The process may be described in the following way. Suppose that lateral imperfections scatter the incident plane wave into spherical waves; these may be decomposed into plane wave components k_{zi} which, for the special values of q_{zM} given above, are reflected by the laterally averaged sample. The relative k_{zM} may be considered as open channels into which the scattered neutrons are allowed to escape. In this pictorial description the constant-k_z scattering results from the sequence of two events, the first the incoherent scattering from lateral imperfections, the second the specular reflectivity from the mean lamellar structure.

Some of the datapoints do not fit along the constant-k_z lines, but instead are aligned along a straight line common to all scattering spectra regardless of the angle of incidence. This line is described by

$$+ k_{zi} = q_{z3} \qquad (2$$

The constant-q_z scattering has also been observed by many authors [3, 10–12] and it has been interpreted in terms of a "conformal roughness". Basically, in this model the multilayer is formed by a sequence of interfaces in registry to each other but not with a reference plane: the multilayer, rather than planar, is wavy or corrugated. In the extremal case the roughness is conformal over the entire thickness of the film, and then the intensity of the scattered radiation at fixed $q_x \neq 0$ has exactly the same q_z dependence of the specularly reflected pattern, up to and including the oscillations due to the total film thickness. If the roughness is conformal over only part of the sample's thickness this correspondence is gradually lost, starting from the total thickness oscillation. In the P(S-b-MMA) sample with layers distorted by the addition of PMMA, not much conformality is expected nor observed. What is observed is that constant-k_z and constant-q_z types of ridges coexist. At their intersection, band structure effects are visible, indicating that some kind of interaction takes place between different modes. Only one constant-q_z ridges is clearly marked. In other samples, instead, the diffuse scattering is preponderantly along constant-q_z lines, as it will be shown in an example drawn from research on magnetic samples.

3. Magnetic multilayers

Magnetic multilayers are made of a periodic sequence of couples, formed by a layer of ferromagnetic metal (Fe, Co, Ni or a rare earth), a few tens of Angstroms thick, followed by a layer of nonmagnetic metal, or spacer, of a given thickness. First for very selected couples, then for a rapidly expanding host of combinations, it was found that the coupling between subsequent ferromagnetic layers oscillates from ferromagnetic to antiferromagnetic to ferromagnetic again as the thickness of the nonmagnetic spacers is increased [13–15]. The nature of the coupling, *inferred* from the magnetization measurements, was first directly observed by neutron reflection. In all recorded cases the alignment of the magnetization of the subsequent layer was either ferromagnetic (F) or antiferromagnetic (AF) of the type $+ - + -$, with a simple doubling of the chemical periodicity. The AF state can be suppressed by a saturating magnetic field. Examples of magnetic multilayers studied by neutron reflection comprise Fe/Cr, Co/Ru, Ni/Ag, Co/Cu and Fe/Nb [16].

Sizeable forward scattering has been almost universally observed in sputtered samples of magnetic multilayers in the AF state [17]. In Fig. 3 is shown the intensity contour map of Fe/Cr multilayers [18] in the q_x, q_z plane. The forward scattering has the form of a ridge of constant-q_z centered around the AF peak. In contrast, at the first Bragg reflection of the modulated chemical structure no diffuse components are present. The forward scattering is of magnetic origin, as if the antiferromagnetic domains had finite size. To describe the magnetic configuration it is sufficient to think the multilayer to be divided into columnar domains. The sublattice magnetization of each domain is totally defined by the orientation of the magnetic moments in the

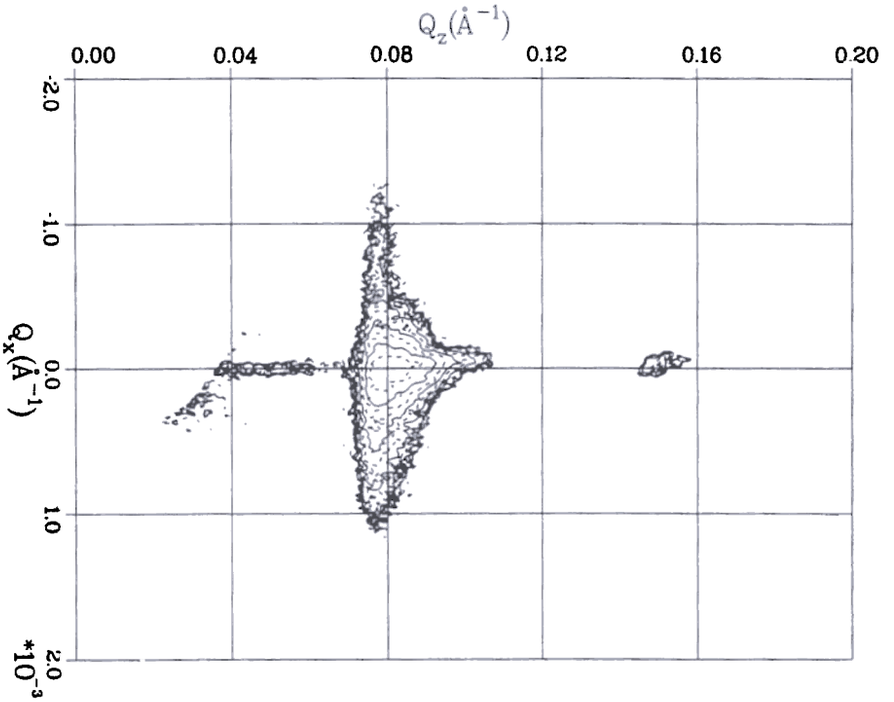

Fig. 3. Contour plot of the neutron intensities forwardly scattered from a sputtered multilayer of Fe/Cr. The thickness of the Fe layers is 30 Å, that of Cr is 10 Å. The magnetic structure is antiferromagnetic, and it gives rise to the intensity scattered at $q_z \sim 0.075$ Å^{-1}. At twice this value the Bragg reflection due to the modulation in material composition is visible.

surface layer. In the absence of an external magnetic field, these moments are likely to point along one of the equivalent crystallographic axes.

The lateral dimensions of the domains observed for Fe/Cr can be calculated with the help of a simple formula. In the kinematic approximation the diffuse intensity around the antiferromagnetic peak is [16]

$$J_x J_z = \frac{\sin^2(N_z a_z q_z/2)}{\sin^2(a_z q_z/2)} \frac{\sin^2(N_x a_x q_x/2)}{\sin^2(a_x q_x/2)} \tag{3}$$

Fluctuations along y were omitted. In Eq. (3), a is the antiferromagnetic spacing and N_z is the number of layers composing the film. a_x is a dummy parameter and what is of interest in the x direction is the total length $L_x = N_x a_x$. At the Bragg reflection $q_x = 0$ and the arguments in J_z are multiples of 2π. When the incident wave vector $k = 2\pi/\lambda$ is changed (but the angle of incidence θ_i remains constant) the maximum of J_z occurs always for the same value of q_z. Under this condition the exit beam makes an angle $\theta_f \neq \theta_i$ with the surface and q_x becomes finite. At the onset of q_x, J_x rapidly decreases; L_x may be chosen by finding the value of q_x at which $J_x = 0$. For instance, for the sample of Fe/Cr giving rise to the scattering of Fig. 3, $L_x \sim 0.4$ μm.

4. Discussion

The diffuse scattering of magnetic multilayers is characterized by a constant-q_z ridge and yet is not due to conformal roughness. Drawing an analogy with conventional crystallography, conformal roughness merely distorts a single crystal; instead, the antiferromagnet is composed of a collage of crystallites. It would be interesting to ascertain the

legitimacy of the multidomain model from the detailed q_x dependence of the scattered intensity. However, such an analysis would require magnetic multilayers in which the distribution of domains was more uniform than in the present sample.

In summary, some aspects were shown of the forward scattering of imperfect multilayers. From the time of Yoneda's observations a robust work of development has taken place [19–21] to explain the features of forward scattering in terms of the distorted wave Born approximation. For multilayers such an approach might be unwieldy except for a few model systems. In an attempt to synthesize the main features of the forward scattering [22], contour plots were presented both in q_x, q_z and θ, λ coordinates. In the same scale the topology of the maxima of the forward scattered neutrons was presented. This last display may turn out to be a useful board to test both the approximations to the scattering theory and the model structural imperfections to which link the observations.

References

[1] J. Penfold and R.K. Thomas, J. Phys. C 2 (1990) 1369.
[2] T.P. Russell, Mater. Sci. Rep. 5 (1990) 171.
[3] S.K. Sinha, Physica B 173 (1991) 25.
[4] M. Tolan, G. König, L. Brügemann, W. Press, F.B. Brinkop and J.P. Kotthaus, Europhys. Lett. 20 (1992) 223.
[5] A. Karim, B.H. Arendt, R. Goyette, Y.Y. Huang, R. Kleb and G.P. Felcher, Physica B 173 (1991) 17.
[6] G. Coulon, T.P. Russell, V.R. Deline and P.F. Green, Macromolecules 22 (1989) 2581.
[7] S.H. Anastasiadis, T.P. Russell, S.K. Satija and C.F. Majkrzak, Phys. Rev. Lett. 62 (1989) 1852; J. Chem Phys. 92 (1990) 5677.
[8] G.P. Felcher, R.J. Goyette, S. Anastasiadis, T.P. Russell, M. Foster and F. Bates, Phys. Rev. Lett., submitted.
[9] Y. Yoneda, Phys. Rev. 131 (1963) 2010.
[10] D.G. Stearns, J. Appl. Phys. 71 (1992) 4286.
[11] D. Bahr, W. Press, R. Jebasinski and S. Mantl, Phys. Rev. B 47 (1993) 4385.
[12] Y.H. Phang, D.E. Savage, R. Kariotis and M.G. Lagally, J. Appl. Phys., to be published.
[13] P. Gruenberg, R. Schreiner, Y. Pang, M.B. Brodsky and H. Sowers, Phys. Rev. Lett. 57 (1986) 2442.
[14] M.N. Baibich, J.M. Broto, A. Fert, F. Nguyen van Dau, F. Petroff, P. Etienne, G. Creuzet and A. Friederich, Phys. Rev. Lett. 61 (1988) 2472.
[15] S.S.P. Parkin, N. More and K.P. Roche, Phys. Rev. Lett. 64 (1990) 2304.
[16] G.P. Felcher, Physica B 192 (1993) 137.
[17] Y.Y. Huang, G.P. Felcher and S.S.P. Parkin, J. Magn. Magn. Mater. 99 (1991) L31.
[18] W. Hahn, M. Löwenhaupt, Y.Y. Huang, G.P. Felcher and S.S.P. Parkin, J. Appl. Phys., to be published.
[19] A. Steyerl, Z. Phys. 254 (1972) 169.
[20] S.K. Sinha, E.B. Sirota, S. Garoff and H.B. Stanley, Phys. Rev. B 38 (1988) 2297.
[21] R. Pynn, Phys. Rev. B 45 (1992) 602.
[22] J.B. Kortright, J. Appl. Phys. 70 (1991) 3620.